Letter

Directing role of pH and ethanol vapour on the formation of 2D or 3D mesostructured silica and hybrid organo-silica thin films

Bruno Alonso,*[a] A. Ruud Balkenende,[b] Pierre-Antoine Albouy,[c] Dominique Durand[d] and Florence Babonneau[e]

[a] *CRMHT, CNRS UPR 4212, 1D av. de la Recherche Scientifique, 45071, Orléans Cedex 2, France. E-mail: alonso@cnrs-orleans.fr; Fax: 33 2 38 63 81 03; Tel: 33 2 38 25 76 82*
[b] *Philips Research Laboratories, Prof. Holstlaan 4, 5656 AA, Eindhoven, Netherlands*
[c] *Laboratoire de Physique des Solides, Université Paris-Sud, 91405, Orsay Cedex, France*
[d] *LURE, bât. 209D, Centre Universitaire, BP 34, 91898, Orsay Cedex, France*
[e] *Laboratoire Chimie de la Matière Condensée, Université Paris VI, 75252, Paris Cedex 05, France*

Received (in Montpellier, France) 4th June 2002, Accepted 16th July 2002
First published as an Advance Article on the web 28th August 2002

A simple synthetic route leading to ordered mesostructured silica and organo-silica thin films is investigated by *in situ* X-ray experiments. The mesophase directing role of pH and of ethanol vapour pressure during film formation is demonstrated. Modifications of these two parameters during dip coating results in three different 2D or 3D mesostructures (*p6mm*, $P6_3/mmc$, or *Pm*3*n*).

Since the discovery of synthetic routes to ordered mesoporous bulk materials,[1] it has been shown that thin films can be obtained by adapting simple sol–gel processes such as spin coating[2] or dip coating[3] in what is called *evaporation induced self-assembly* (EISA).[4] Based on rapid solvent evaporation that promotes the formation of a mesophase between surfactants and oligomers initially present at low concentrations, this concept is of widespread use for thin film formation. By varying the experimental conditions (reactants, solvent, ionic strength, *etc.*), it is possible to broaden the accessible ranges of porosity, mesostructures, oxide networks and added functionalities. In the case of silica, various 2D or 3D mesophases have been formed[5,6] and organic groups with various functionalities have been successfully introduced.[7] However, there is still a need for mechanistic studies allowing a better understanding of the underlying and determining phenomena: evaporation (and other transfers at the air–film interface like adsorption), mesophase formation (and related surfactant aggregation phenomena), and network formation (condensation and aggregation of oligomers). These phenomena are themselves governed by various parameters belonging to the experimental conditions. In order to develop mesoporous films with the desired properties, the most determining parameters need to be properly identified and controlled. Our work was aimed in this direction, in an attempt to combine the richness of the EISA process with reproducibility.

A previous work on water-rich starting sols[8] correlated the nature of the mesophases formed by dip coating for alkyltrimethylammonium surfactants and silicate oligomers to those obtained at the same surfactant volume fraction in pure water. This cannot explain the formation of 3D hexagonal or cubic mesophases obtained with the same technique and the same reactants in ethanol-rich sols.[6,9] In addition, it has been shown that the condensation degree of the silicate oligomers in the starting sols is an important parameter for the formation of ordered silica films, but not so crucial as it can take very different values for films having same final mesostructures, or similar values for films with different mesostructures.[9] In this letter, we present new results based on *in situ* X-ray diffraction (XRD) measurements that lead to new insights in the mechanisms of formation of ordered mesostructured silica and organo-silica thin films. In particular, we emphasises the role of pH and of ethanol vapour concentration during dip coating in determining the final mesostructures.

Similar results were obtained for the silica and the organo-silica films. As described previously, we noticed only small differences in the effect of sol ageing and in the value of inter-reticular distances.[9] The replacement of 20% of the starting precursor tetraethoxysilane (TEOS) by methyl- or phenyltriethoxysilane (MTES or PTES) has here little influence on the self-assembly processes. This could be explained by the existence of much more directing parameters, such as pH and dip coating conditions. For the less acidic sols (aqueous HCl 10^{-2} M solution), only the 2D hexagonal mesophase (plane group *p6mm*) was observed (Fig. 2b) with a preferential orientation of {01} planes parallel to the substrates (*x* axis) as noticed in previous works.[10] This mesophase appears within the first minute after deposition, and ageing of the film leads to an unidirectional contraction.

With more acidic sols (HCl 10^{-1} M), different behaviour is noticed. At short ageing times of the sols (from 2 to 24 h) the 3D hexagonal mesophase (space group $P6_3/mmc$) with a preferential orientation of {002} planes parallel to the substrates[6] is always obtained. For longer ageing times of the sols, and depending on dip coating conditions (Fig. 1a), either this mesophase (condition A) or a cubic mesophase (space group $Pm(-3)n$, typed here *Pm*3*n*) with {211} planes parallel to the substrate (condition B) can be obtained (Fig. 2c, 2d). During *in situ* experiments, we observed that in fact the 3D hexagonal mesophase is always formed within the first minute for various sols aged from 35 h up to 175 h (this last case corresponding to TEOS as the only silicon alkoxide). By using dip coating condition A, this mesophase is then retained and no other mesophase was observed, whereas by using condition B, a phase transition towards the cubic phase occurs in the following minute (Fig. 3).

From XRD patterns, we noticed that several diffraction peaks from $P6_3/mmc$ and *Pm*3*n* mesophases are close in position during the phase transition (circled in Fig. 3) although

DOI: 10.1039/b205501p

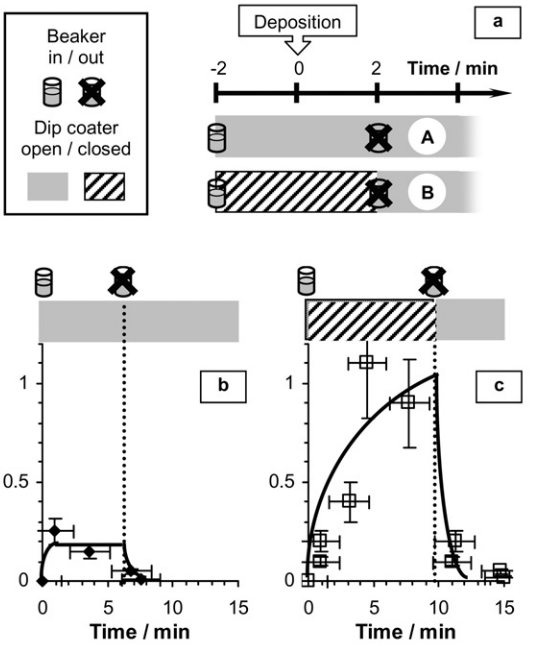

Fig. 1 (a) Dip coating conditions employed. Variations of EtOH vapour percentage inside the dip coater as a function of time when: (b) the dip coater is always open; (c) the dip coater is closed until the beaker containing the sol is removed. Lines are guides for the eye.

not overlapping. As no simple relationship between crystallographic planes has been found until now, epitaxial growth is not expected. The transition may thus proceed by small deformations of the arrangement of aggregates in various directions. Similar comments have been made for this transition in the case of the binary $C_{12}EO_8$–water phase diagram.[11] In that case, with increasing surfactant concentrations and aggregation number, and thus decreasing the curvature of the micellar aggregates, the phases $P6_3/mmc$, *Pm*3*n* and *p*6*mm* were successively observed.

In the case presented here (Fig. 3), the transition from $P6_3/mmc$ to *Pm*3*n* mesophases, observed only for dip coating condition B, occurs one minute or more after deposition, and thus more than 30 seconds after the end of the evaporation step. Therefore, a direct link of causality between the evaporation of EtOH and this transition is missing. This is also supported by the fact that mass losses of the sols as a function of time were almost constant (around 6.5 10^{-3} g min^{-1}) for both dip coating conditions. In contrast, measurements of EtOH vapour volumetric percentages inside the dip coater obtained in similar experiments showed strong variations during a timescale long enough to favour the transition (Fig. 1b, c). We can estimate that before the removal of the beaker, *ca.* 0.2 vol.% EtOH is present for condition A, while this is *ca.* 0.8 vol.% for condition B. Afterwards, EtOH concentration decreases in both cases down to less than 0.01%. There is thus a strong relationship between high EtOH vapour concentrations inside the dip coater and the phase transition from $P6_3/mmc$ to *Pm*3*n*.

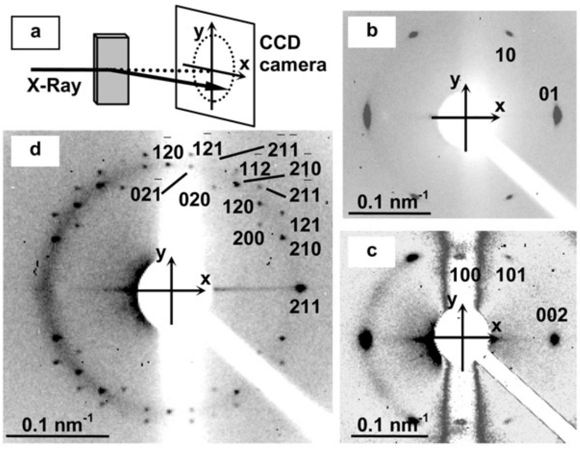

Fig. 2 (a) Experimental setup for *in situ* XRD analysis. XRD patterns of films obtained from: (b) a sol TEOS:PTES:CTAB:EtOH:HCl 10^{-2} M (0.8:0.2:0.12:20:5) aged 40 h (conditions B, *p*6*mm*), (c) a sol TEOS:CTAB:EtOH:HCl 10^{-1} M (1:0.12:20:5) aged 160 h (conditions A, $P6_3/mmc$), and (d) a sol TEOS:MTES:CTAB:EtOH:HCl 10^{-1} M (0.8:0.2:0.12:20:5) aged 40 h (conditions B, *Pm*3*n*).

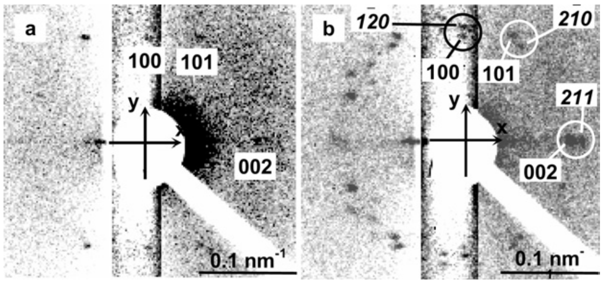

Fig. 3 Deposition of a sol TEOS:CTAB:EtOH:HCl 10^{-1} M (1:0.12:20:5) aged 37 h and using dip coating condition B. XRD patterns (exposure time: 1 min) were recorded: (a) from 0 to 1 min after deposition ($P6_3/mmc$), (b) from 1 to 2 min after deposition ($P6_3/mmc$, *Pm*3*n*). No other mesophase transition was observed at longer times. Indexation of peaks of the *Pm*3*n* mesophase is done using italic numbers. In order to visualise all the diffraction peaks, two levels of contrast were used in the images.

A particular role of EtOH in other phase transitions has been noticed in precipitated mesoporous silicates.[12] Here, the EtOH concentration in the film is monitored by the exchange of matter at the air–film interface. At the beginning of the deposition, EtOH is the major component of the film and it evaporates largely in the first seconds of dip coating (observation of interference fringes) irrespective of the concentration of EtOH vapour inside the dip coater. This promotes surfactant aggregation and mesophase formation that may be kinetically controlled. After this evaporation step, stresses in the film are large and the viscosity increases sharply until solidification as for classical oligomeric sols[13] although the presence of mesophases slows down these processes.[4] However, at high vapour EtOH concentrations (condition B) a relatively high level of EtOH is maintained within the film.† In this case, the films remain low in viscosity, opening the way to phase transitions, in contrast to what happens in less ethanol-rich atmospheres (condition A). In addition, the presence of EtOH will delay condensation reactions and thus network formation and solidification. However, EtOH as a water co-solvent is known to decrease the polarity of the medium leading to a decrease of the aggregative properties,[14] and this is somehow difficult to relate to the promotion of mesophases with less curvature.

Differences between the final mesostructures obtained using different HCl aqueous solutions are also difficult to explain. In previous work,[5] it was argued that higher HCl concentrations will favour stronger interactions between silicate oligomers and assemblies of surfactants (in this case, cetyltriethylammonium bromide CTEAB), leading to 2D *p*6*mm* mesophases instead of 3D *Pm*3*n*. In contrast, we observed, for a given condensation degree between siloxane species (measured by ^{29}Si liquid-state NMR) that *p*6*mm* mesophases are formed using HCl 10^{-2} M, and $P6_3/mmc$ or *Pm*3*n* mesophases using HCl 10^{-1} M. The two latter mesophases are not observed in

---

† Intensive exposure to EtOH vapour can even dissolve completely an as-deposited film.

CTAB–water–EtOH phase diagrams. However, the $Pm3n$ mesophase can be promoted by moving to a less polar solvent and to other counter ions.[15] We suspect that differences in HCl content should also lead to differences in EtOH content. Indeed, the protonation of EtOH may favour higher EtOH concentrations in the film and thus a less polar medium. In addition, the interaction between siloxane oligomers and CTA^+ surfactants will be modified due to the differences in the extent of protonation of silanol groups. Further, a useful but hardly accessible parameter, similarly important as the condensation degree and also dependent on the pH, is the distribution in size of these siloxane oligomers. This distribution will influence the viscosity of the film as well as the interaction with surfactant assemblies.

In conclusion, this preliminary work demonstrates the directing role in mesophase formation of two parameters often neglected: pH and ethanol vapour concentration during film formation. However, these parameters may be at the origin of some problems of reproducibility, but also of the richness of the EISA process.‡ In order to investigate exhaustively these aspects of mesophase formation, more data could be obtained through other spectroscopic techniques such as infra-red, allowing information on size distributions of the siloxane oligomers to be obtained, and fluorescence, using molecular probes sensitive to the polarity and viscosity of the media. Such work is in progress.

Experimental

Ordered mesostructured thin films were obtained after ageing and dip coating of sols. Sols were simply prepared by mixing together silicon alkoxides, cetyltrimethylammonium bromide (CTAB), ethanol (EtOH) and an aqueous HCl solution (10^{-1} or 10^{-2} M) in 1:0.12:20:5 molar proportions. If the silicon alkoxide is tetraethoxysilane (TEOS), inorganic silica films are formed, whereas using TEOS mixed in 0.8:0.2 molar proportions to methyltriethoxysilane (MTES) or to phenyltriethoxysilane (PTES) leads to hybrid organo-silica films. Sols ($n_{Si} = 10^{-2}$ mol) were aged at room temperature in closed vessels and under stirring (500 rpm). Ageing times can be varied from 2 h to 10 days. Afterwards, sols were deposited by dip coating on 20 μm thick silicon substrates, needed for *in situ* X-ray measurements.

The dip coater designed for *in situ* measurements was relatively small (20 cm height, 5 cm width, 20 cm depth) with an air capacity of *ca.* 2 L and could be used either in an opened state, *i.e.* allowing for vapour exchange with the environment, or in a closed state. The substrate is in a fixed position and the beaker is moved up and down at a rate of 9 cm min^{-1}. Two types of dip coating conditions (A and B) were used in this work (Fig. 1a). The dip coater was either open during the entire experiment (A), or closed after placing the beaker containing the sol and opened when the beaker is removed (B). The beaker (top surface of 4.9 cm^2) is placed two minutes before film deposition and removed two minutes later. Inside the dip coater, measured temperature and humidity were in the 24–27 °C and 34–42% RH ranges. The volumetric percentage of EtOH vapour was measured by air sampling using calibrated test tubes (Merck). XRD patterns were recorded after film deposition in near grazing angle incidence (Fig. 2a) at a SAXS beam line using synchrotron radiation (LURE, France). For each dip coating experiment, the end of the solvent evaporation step[13] was controlled by interferometry using a monochromatic lamp. We observed it at 15 ± 5 s after withdrawal of the substrate from the solution.

Acknowledgements

We thank Gregor Trimmel for his help during X-ray measurements. This work was funded by Philips Electronics (Eindhoven, The Netherlands).

References

1 C. T. Kresge, M. E. Leonowicz, W. J. Roth, J. C. Vartuli and J. S. Beck, *Nature*, 1992, **359**, 710.
2 M. Ogawa, *J. Am. Chem. Soc.*, 1994, **116**, 7941.
3 Y. Lu, R. Ganguli, C. A. Drewien, M. T. Anderson, C. J. Brinker, W. Gong, Y. Guo, H. Soyez, B. Dunn, M. H. Huang and J. I. Zink, *Nature*, 1997, **389**, 364.
4 C. J. Brinker, Y. Lu, A. Sellinger and H. Fan, *Adv. Mater.*, 1999, **11**, 579.
5 D. Zhao, P. Yang, D. I. Margolese, B. F. Chmelka and G. D. Stucky, *Chem. Commun.*, 1998, 2499.
6 (*a*) S. Besson, T. Gacoin, C. Jacquiod, C. Ricolleau, D. Babonneau and J.-P. Boilot, *J. Mater. Chem.*, 2000, **10**, 1331; (*b*) D. Grosso, A. R. Balkenende, P.-A. Albouy, M. Lavergne, L. Mazerolles and F. Babonneau, *J. Mater. Chem.*, 2000, **10**, 2085; (*c*) D. Grosso, F. Babonneau, G. J. de A. A. Soler-Illia, P.-A. Albouy and H. Amenitsch, *Chem. Commun.*, 2002, 748.
7 (*a*) A. Sellinger, P. M. Weiss, A. Nguyen, Y. Lu, R. A. Assink, W. Gong and C. J. Brinker, *Nature*, 1998, **394**, 256; (*b*) Y. Lu, H. Fan, N. Doke, D. A. Loy, R. A. Assink, D. A. LaVan and C. J. Brinker, *J. Am. Chem. Soc.*, 2000, **122**, 5258.
8 M. Klotz, A. Ayral, C. Guizard and L. Cot, *J. Mater. Chem.*, 2000, **10**, 663.
9 B. Alonso, A. R. Balkenende, P.-A. Albouy, H. Amenitsch, M.-N. Rager and F. Babonneau, *J. Sol–Gel Sci. Technol.*, in press.
10 M. Klotz, P.-A. Albouy, A. Ayral, C. Ménager, D. Grosso, A. Van der Lee, V. Cabuil and C. Guizard, *Chem. Mater.*, 2000, **12**, 1721.
11 M. Clerc, *J. Phys. II (France)*, 1996, **6**, 961.
12 (*a*) K. W. Gallis and C. C. Landry, *Chem. Mater.*, 1997, **9**, 2035; (*b*) C. C. Landry, S. H. Tolbert, K. W. Gallis, A. Monnier, G. D. Stucky, P. Norby and J. C. Hanson, *Chem. Mater.*, 2001, **13**, 1600
13 (*a*) C. J. Brinker and G. W. Scherer, *Sol–Gel Science*, Academic Press, San Diego, 1990; (*b*) C. J. Brinker, G. C. Frye, A. J. Hurd and C. S. Ashley, *Thin Solid Films*, 1991, **201**, 97.
14 R. Zana, *Adv. Colloid Interface Sci.*, 1995, **57**, 1.
15 X. Auvray, M. Abiyaala, P. Duval and C. Petipas, *Langmuir*, 1993, **9**, 444.

---

‡ As an example, we find that under special dip coating conditions a sol gives a predominant $P6_3/mmc$ mesostructure at one face of the substrate and a predominant $Pm3n$ mesostructure at the other face.